Final-state effects on superfluid ^{4}He in the deep inelastic regime

F. Mazzanti

Departament d'Estructura i Constituents de la Matèria, Diagonal 645, Universitat de Barcelona, E-08028 Barcelona, Spain

J. Boronat

Departament de Física i Enginyeria Nuclear, Campus Nord B4-B5, Universitat Politècnica de Catalunya, E-08028 Barcelona, Spain

A. Polls

Departament d'Estructura i Constituents de la Matèria, Diagonal 645, Universitat de Barcelona, E-08028 Barcelona, Spain

A study of final-state effects (FSE) on the dynamic structure function of superfluid ^{4}He in the Gersch-Rodriguez formalism is presented. The main ingredients needed in the calculation are the momentum distribution and the semidiagonal two-body density matrix. The influence of these ground-state quantities on the FSE is analyzed. A variational form of ρ_2 is used, even though simpler forms turn out to give accurate results if properly chosen. Comparison to the experimental response at high momentum transfer is performed. The predicted response is quite sensitive to slight variations on the value of the condensate fraction, the best agreement with experiment being obtained with $n_0 = 0.082$. Sum rules of the FSE broadening function are also derived and commented. Finally, it is shown that Gersch-Rodriguez theory produces results as accurate as those coming from other more recent FSE theories.

I. INTRODUCTION

Deep inelastic neutron scattering (DINS) has been extensively applied to the study of quantum fluids, since Hohenberg and Platzman's[1] proposal of using DINS to determine the momentum distribution $n(k)$ of helium atoms in superfluid ^{4}He. The determination of $n(k)$ in quantum liquids is a challenging problem of fundamental interest.[2] In fact, the knowledge of $n(k)$ provides very useful information to understand basic properties of the quantum nature of these systems as the Bose-Einstein condensation. At the same time, the theoretical analysis of DINS probes and stimulates the development of modern many-body techniques. These issues have been the main motivations of a considerable amount of measurements and theoretical work on liquid ^{4}He and other quantum liquids.[3–17]

The inelastic scattering of neutrons by liquid ^{4}He is described by the double differential cross section

$$\frac{d^2\sigma}{d\Omega d\omega} = b^2 \frac{k_f}{k_i} S(q,\omega), \qquad (1)$$

where b is the scattering length, k_i and k_f are the initial and final wave vectors of the scattered neutron, and q and ω are the momentum and energy transferred from the neutron to the sample. The dynamics of the sample is entirely contained in $S(q,\omega)$, the dynamic structure factor, which is the Fourier transform of the density-density correlation function.[18] At sufficiently high momentum transfer, the scattering is entirely due to single atoms and $S(q,\omega)$ can be accurately described by the impulse approximation (IA),[1] provided that the interatomic potential does not have an infinite repulsive core. In this regime, the kinetic energy of an atom recoiling from a neutron collision is much larger than the potential energy due to the interaction with the neighboring atoms, so

that collisions of the former with other atoms can be neglected. The IA predicts a simple relation between $S(q,\omega)$ and $n(k)$,

$$S_{\mathrm{IA}}(q,\omega) = \frac{1}{(2\pi)^3\rho} \int d\mathbf{k} \; n(k)\delta\left(\omega - \omega_R - \frac{\mathbf{k}\cdot\mathbf{q}}{m}\right), \quad (2)$$

where $\omega_R = q^2/2m$ is the free atom recoil frequency, m is the mass of the ^{4}He atoms, and $n(k)$ is the thermally averaged occupation probability of the single particle state of momentum $\mathbf{k}$, which reduces to that of the ground state at $T=0$. The delta function in Eq. (2) takes care of the momentum and energy conservation in the scattering event between the neutron and a single atom. Assuming $S(q,\omega) = S_{\mathrm{IA}}(q,\omega)$, the momentum distribution $n(k)$ can be extracted from Eq. (2) by simple differentiation. Notice that in the previous equation and henceforth $\hbar$ is set to 1.

In isotropic systems, where $n(k)$ depends only on the modulus of $\mathbf{k}$, it is useful to introduce the Compton profile

$$J_{\mathrm{IA}}(Y) = \frac{q}{m} S_{\mathrm{IA}}(q,\omega), \qquad (3)$$

which is driven by a single variable

$$Y = \frac{m}{q}\left(\omega - \frac{q^2}{2m}\right), \qquad (4)$$

and fulfills Y scaling.[19] If a finite fraction of atoms n_0 occupies the zero momentum state, $J_{\mathrm{IA}}(Y)$ presents a δ peak of strength n_0 at $Y=0$. However, this expected signature of the condensate is not observed in experiments performed at momentum transfer as high as 23 Å^{-1},[4] because the IA spectrum is broadened by both final-state effects (FSE) and instrumental resolution effects (IRE). Hence the theoretical interpretation of the experimental data requires not only the

knowledge of $n(k)$, but also an accurate description of both the dynamics which determines FSE and the instrumental broadening function.[5]

Several methods to account for FSE have been proposed.[8,9,12–15] Among them, we will focus on the so-called convolutive theories, in which

$$S(q,\omega) = \int_{-\infty}^{\infty} d\omega' \, S_{\mathrm{IA}}(q,\omega') R(q,\omega-\omega'), \qquad (5)$$

where $R(q,\omega)$ is the FSE broadening function.

After the first attempt[1] to approximate $R(q,\omega)$ by a Lorentzian of width proportional to the ^{4}He-^{4}He cross section, Gersch et al.[8] expressed the response function $S(q,\omega)$ in a $1/q$ series expansion, whose coefficients are given by integrals of many-body correlation functions averaged on the ground state of the system. In this approach, the response when $q \to \infty$ is given by the first term of the expansion of the incoherent part of $S(q,\omega)$, which turns to be exactly the IA. However, the theory could not deal with realistic interatomic potentials presenting a strong repulsion at short distances. To overcome this problem, Gersch and Rodriguez[9] proposed a cumulant expansion of $S(q,t)$ which provides an adequate frame for calculating the response function at high momentum transfer. The full calculation is impractical, but with some approximations based on physical grounds, $S(q,\omega)$ can be expressed in terms of the one- and the semidiagonal two-body density matrices, and the two-body interaction. At the time the theory was proposed the numerical application was made with a very simple approximation of the two-body density matrix that resulted in an overestimation of the response at the quasielastic peak.[10]

The main purpose of the present work is to revisit Gersch-Rodriguez theory, and show that using a realistic two-body density matrix one gets a $S(q,\omega)$ in good agreement with both experimental data and more recent theories of FSE.[12,14]

In the next section, a review of the theory is presented. Section III is devoted to the discussion of the results and their comparison with the experimental data. A sum rules analysis of $R(q,\omega)$ is presented in Sec. IV. In Sec. V our results are compared with other FSE theories, and finally Sec. VI summarizes the main conclusions of the work.

II. GERSCH-RODRIGUEZ THEORY OF FSE

In the Gersch-Rodriguez theory,[9] the density-density correlation factor $S(q,t)$ is expressed as the product of the IA and the FSE correcting function by means of a cumulant expansion. The nth order cumulant accounts for the correlations among the struck atom and clusters of n particles in the background. In the high momentum transfer limit, those terms with $n=1$ carry the most significant corrections. At this level, the FSE broadening function can be expressed as a function of the interatomic potential and the one- and two-body density matrices.

The starting point in Gersch-Rodriguez theory is the time representation of the response

$$NS(q,t) = \sum_{j,l} \langle e^{-i\mathbf{q}\mathbf{r}_l} e^{iHt} e^{i\mathbf{q}\mathbf{r}_j} e^{-iHt} \rangle$$

$$= \sum_{j,l} \langle e^{i\mathbf{q}(\mathbf{r}_j - \mathbf{r}_l)} e^{-i\mathbf{q}\mathbf{r}_j} e^{iHt} e^{i\mathbf{q}\mathbf{r}_j} e^{-iHt} \rangle, \qquad (6)$$

which can be brought to the following form:

$$NS(q,t) = e^{i\omega_q t} \sum_{j,l} \left\langle e^{i\mathbf{q}(\mathbf{r}_j - \mathbf{r}_l)} e^{iL_j t} \right.$$

$$\left. \times T \exp\left[i \int_0^t dt' \, H(\mathbf{r}_j - \mathbf{v}_q t') \right] e^{-iHt} \right\rangle, \qquad (7)$$

where T is the time-ordering operator and $H(\mathbf{r}_j - \mathbf{v}_q t')$ is the actual Hamiltonian of the system where the position coordinate of particle j has been shifted by an amount $\mathbf{v}_q t'$. As the interatomic potential considered is velocity independent, one can write

$$H(\mathbf{r}_j - \mathbf{v}_q t') = H + U_j(\mathbf{v}_q t'), \qquad (8)$$

with

$$H = \sum_j \frac{p_j^2}{2m} + \sum_{i<j} V(r_{ij}) \qquad (9)$$

and

$$U_j(\mathbf{v}_q t') = \sum_{m \neq j} U_{j,m}(v_q t'),$$

$$U_{j,m}(v_q t') = [V(\mathbf{r}_j - \mathbf{v}_q t', \mathbf{r}_m) - V(\mathbf{r}_j, \mathbf{r}_m)], \qquad (10)$$

where $v_q = q/m$ and $\omega_q = q^2/2m$.

The incoherent part of the response, which is defined by taking particles labeled j and l in Eq. (7) to be the same, is the only contribution at large q. In this limit, $S(q,t)$ may be written in the following way:

$$S(q,t)$$

$$= e^{i\omega_q t} \left\langle e^{i\mathbf{v}_q t \mathbf{p}_1} e^{iHt} T \exp\left[i \int_0^t dt' \sum_{m \neq 1} \hat{U}_{1,m}(\mathbf{v}_q t') \right] e^{-iHt} \right\rangle, \qquad (11)$$

where $\hat{U}(\mathbf{v}_q t')$ is the previously defined potential operator but with the position operators evaluated at time t' rather than at $t=0$. Notice that expression (11) is as hard to evaluate as the original $S(q,t)$. An exact treatment would require the knowledge of the time evolution of the whole system, so different approximations should be made in order to deal with this last relation.

Gersch and Rodriguez[9] performed a cumulant expansion of the ground-state expectation value of Eq. (11). The expansion contains an infinite number of terms, and allows for the factorization of the IA from the total response

$$S(q,t) = S_{\mathrm{IA}}(q,t) R(q,t), \qquad (12)$$

$R(q,t)$ being the FSE correcting function given by

$$R(q,t) = \exp\left[-\frac{1}{\langle e^{it\mathbf{v}_q\mathbf{p}_1}\rangle} \sum_{m\neq 1} \left\langle e^{it\mathbf{v}_q\mathbf{p}_1} \right.\right.$$

$$\left.\left. \times \left[1 - T\exp\left\{ i\int_0^t dt' \hat{U}_{1,m}(\mathbf{v}_q t') \right\} \right] \right\rangle + \cdots \right]. \quad (13)$$

Up to this point, the result is exact because it is nothing more than a rearrangement of the different terms entering in $S(q,t)$. The first problem in the calculation of Eq. (13) is associated to the infinite number of terms appearing in the exponential. Such a difficulty can be skipped if one looks for the underlying physics contained in each term: the contribution of the nth order cumulant to $S(q,t)$ accounts for the correlations between n-particle clusters during their interactions with the struck atom. One may expect that the first significant correction to the IA is produced by the multiple scattering of the struck particle with the atoms of the media, considering them independently of each other. This corresponds to a truncation of the series beyond the first order cumulant.

The second problem lies on the evaluation of the time dependence appearing in the particle coordinates of $\hat{U}_{1,m}(\mathbf{v}_q t')$. In the large q limit, the displacement of the struck particle is much larger than the average movement of the background atoms. Thus one can discard the time dependence of $\mathbf{r}(t)$ in $\hat{U}_{1,m}$. This is a safe procedure as, even though the inclusion of such a time dependence avoids hardcore collisions between the struck particle and other target atoms, the contribution to $R(q,t)$ coming from those situations vanishes due to rapid oscillations in the imaginary exponential of Eq. (13). Therefore, one can write[9]

$$R(q,t) = \exp\left[-\frac{1}{\rho_1(v_q t)} \int d\mathbf{r}\, \rho_2(\mathbf{r},0;\mathbf{r}+\mathbf{v}_q t,0) \left[1 \right.\right.$$

$$\left.\left. -\exp\left\{ i\int_0^t dt' \{V[\mathbf{r}+\mathbf{v}_q(t-t')] - V[\mathbf{r}+\mathbf{v}_q t]\} \right\} \right] \right],$$

$$(14)$$

where ρ_1 and ρ_2 are the one-body and semidiagonal two-body density matrices of the system, respectively. $R(q,t)$ is a complex function, but its Fourier transform is real because its real part is even and its imaginary part odd under the change $t \rightarrow -t$.

Equation (12) predicts $S(q,t)$ as the product of $S_{IA}(q,t)$ and $R(q,t)$, and therefore $S(q,\omega)$ is the convolution of $S_{IA}(q,\omega)$ and $R(q,\omega)$

$$S(q,\omega) = \int_{-\infty}^{\infty} d\omega'\, S_{IA}(q,\omega') R(q,\omega-\omega'). \quad (15)$$

In the particular case of liquid ^{4}He, the momentum distribution $n(k)$ may be written as

$$n(k) = (2\pi)^3 \rho n_0 \delta(\mathbf{k}) + \tilde{n}(k), \quad (16)$$

where n_0 is the condensate fraction value and $\tilde{n}(k)$ stands for the occupation of nonzero momentum states. Consequently, $S_{IA}(q,\omega)$ is split in two parts

$$S_{IA}(q,\omega) = n_0 \delta\left(\omega - \frac{q^2}{2m} \right) + \frac{m}{4\pi^2 \rho q} \int_{|\frac{m\omega}{q} - \frac{q}{2}|}^{\infty} k n(k)\, dk$$

$$= n_0 \delta\left(\omega - \frac{q^2}{2m} \right) + \tilde{S}_{IA}(q,\omega), \quad (17)$$

where the first term on the right-hand side is the condensate response which appears as a delta peak of strength n_0 located at the quasielastic energy, and $\tilde{S}_{IA}(q,\omega)$ is the noncondensate contribution of $n(k)$ to the IA. Introducing the West variable $Y = m\omega/q - q/2$, $S_{IA}(q,\omega)$ can be expressed in terms of the Compton profile

$$\frac{q}{m} S_{IA}(q,\omega) \equiv J_{IA}(Y) = n_0 \delta(Y) + \frac{1}{4\pi^2 \rho} \int_{|Y|}^{\infty} k n(k)\, dk,$$

$$(18)$$

which scales in Y.

Moreover, at high q the response is usually expressed in terms of Y through the relation

$$J(q,Y) = \frac{q}{m} S(q,\omega), \quad (19)$$

and thus Eq. (15) is transformed into

$$J(q,Y) = \int_{-\infty}^{\infty} dY'\, J_{IA}(Y') R(q,Y-Y')$$

$$= n_0 R(q,Y) + \int_{-\infty}^{\infty} dY'\, \tilde{J}_{IA}(Y') R(q,Y-Y'),$$

$$(20)$$

where

$$R(q,Y) = \frac{q}{m} R(q,\omega). \quad (21)$$

III. NUMERICAL RESULTS

In this section, we present results for the FSE correcting function $R(q,Y)$ and the response function $J(q,Y)$ calculated in the framework of the Gersch-Rodriguez formalism. The input density matrices $\rho_1(r)$ and $\rho_2(\mathbf{r}_1,\mathbf{r}_2;\mathbf{r}_1',\mathbf{r}_2)$ used to calculate $J_{IA}(Y)$ and $R(q,Y)$ have been obtained in the framework of the HNC theory[20,21,23] from a variational many-body wave function containing two- and three-body correlations.[22] The variational minimization has been performed for the HFDHE2 Aziz potential[24] at the experimental equilibrium density ($\rho = 0.365\sigma^{-3}$; $\sigma = 2.556$ Å). The ground-state description obtained with this wave function is in good agreement with recent Green's function Monte Carlo calculations.[25,26] The discussion is separated in two parts, the first one being devoted to the study of both $R(q,Y)$ and $J(q,Y)$ and their comparison to experimental data, and the second one to the analysis of the dependence of these functions on the different approximations used in the variational description of the ground-state wave function.

The actual calculation of the FSE broadening function is initially performed in time representation (14). $R(q,x)$ is a complex quantity which can be written in the following way:
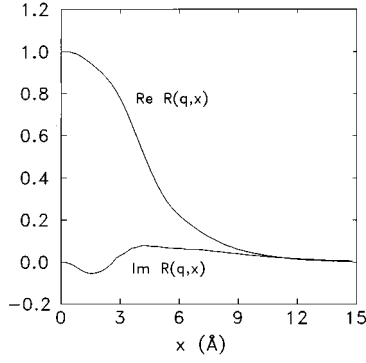
FIG. 1. Real and imaginary parts of $R(q,x)$ at $q=23.1$ Å^{-1}.

$$R(q,x)=e^{\phi(q,x)}[\cos(\psi(q,x))+i\,\sin(\psi(q,x))], \quad (22)$$

with

$$\phi(q,x)=-\frac{2}{\rho_1(x)}\int d\mathbf{r}\,\rho_2(\mathbf{r},0;\mathbf{r}+\mathbf{x})$$
$$\times\sin^2\left[\frac{1}{2v_q}\int_0^x du\{V(\mathbf{r}+\mathbf{x}-\mathbf{u})-V(\mathbf{r}+\mathbf{x})\}\right],$$

$$\psi(q,x)=\frac{1}{\rho_1(x)}\int d\mathbf{r}\,\rho_2(\mathbf{r},0;\mathbf{r}+\mathbf{x})$$
$$\times\sin\left[\frac{1}{v_q}\int_0^x du\{V(\mathbf{r}+\mathbf{x}-\mathbf{u})-V(\mathbf{r}+\mathbf{x})\}\right],$$

$$(23)$$

x being $v_q t$. As can be seen from Eq. (23), $\phi(q,x)$ and $\psi(q,x)$ are even and odd functions of x, respectively. Therefore, the real and imaginary parts of $R(q,x)$ are respectively even and odd under the change $x\rightarrow-x$, and consequently $R(q,Y)$ is real. Even if the potential becomes very repulsive at short distances, as is the case of the Aziz potential, Eq. (14) gives an $R(q,Y)$ which does not diverge.

The real and imaginary parts of $R(q,x)$ are shown in Fig. 1 for $q=23.1$ Å^{-1}. In the relevant range of x, Re$R(q,x)$ has a dominant decreasing behavior. The Re$R(q,x)$ and Im-$R(q,x)$ are related to the symmetric and antisymmetric components of $R(q,Y)$, respectively. As the imaginary part is much smaller than the real part, $R(q,Y)$ is mostly symmetric around $Y=0$. In Fig. 2, we show $\psi(q,x)$ and $\phi(q,x)$ at
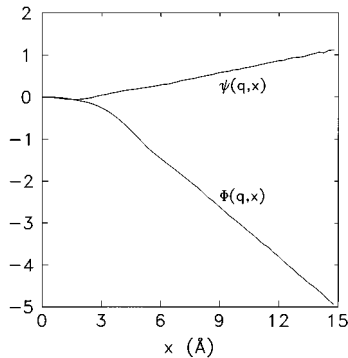

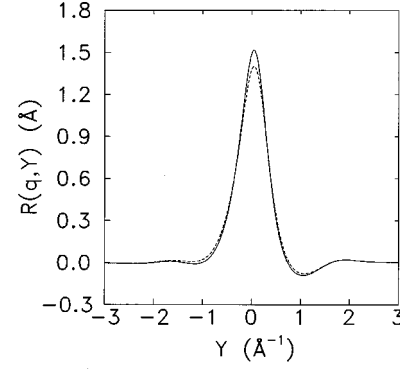FIG. 2. Functions $\phi(q,x)$ and $\psi(q,x)$ at $q=23.1$ Å^{-1}.

FIG. 3. $R(q,Y)$ at $q=23.1$ Å^{-1} (solid line) and $q=15.0$ Å^{-1} (dashed line).

$q=23.1$ Å^{-1}. $\phi(q,x)$ is a negative and a monotonously decreasing function of x, causing both the real and the imaginary parts of $R(q,x)$ tend to zero when $x\rightarrow\infty$ (22).

In Fig. 3, we show $R(q,Y)$ at two different values of q, 23.1 Å^{-1} and 15.0 Å^{-1}. The main trends of $R(q,Y)$ in all FSE convolution theories are the same: a dominant central peak and small oscillating tails which vanish as $|Y|$ increases. As one can see, the shape of $R(q,Y)$ smoothly changes with q, this variation being reflected in an overall redistribution of the strength between the main peak and the wings. When q increases, the peak appears higher and narrower pointing to the tendency of $R(q,Y)$ to become a delta distribution in the limit $q\rightarrow\infty$.

The existence of a finite condensate fraction n_0 in superfluid ^{4}He plays an important role in the FSE corrections, as is reflected in Fig. 4 where the broadening of the condensate and noncondensate parts of $J_{\text{IA}}(Y)$ are separately shown. The small differences between $\tilde{J}_{\text{IA}}(Y)$ (dotted line) and the convolution of $\tilde{J}_{\text{IA}}(Y)$ with $R(q,Y)$ (long-dashed line) reveal small FSE on the noncondensate part of the response at high q. In contrast, the broadening of the condensate term (short-dashed line), i.e., the convolution product of $R(q,Y)$ and $n_0\delta(Y)$, contributes to $J(q,Y)$ as $n_0R(q,Y)$ which is a function with an appreciable width and height. The inclusion of the latter term produces a total $J(q,Y)$ (solid line) which
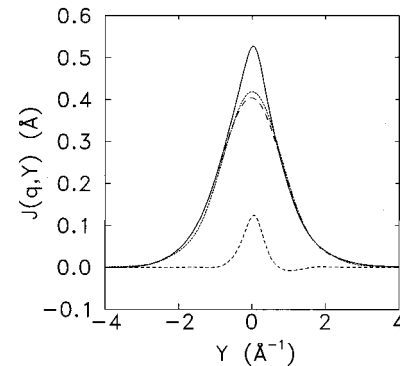

FIG. 4. Different contributions to $J(q,Y)$ at $q=23.1$ Å^{-1}. Dotted line, noncondensate term of $J_{\text{IA}}(Y)$; long-dashed line, noncondensate term of $J_{\text{IA}}(Y)$ after the convolution with $R(q,Y)$; short–dashed line, condensate contribution once broadened by FSE; solid line, total response.
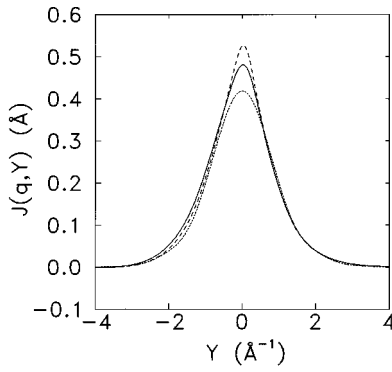
FIG. 5. Effects of the different broadenings to the response at $q = 23.1$ Å^{-1}. Dotted line, noncondensate IA prediction; dashed line, IA broadened by FSE; solid line, total $J(q,Y)$ including both FSE and IRE.

manifests a sizeable departure from the IA prediction. Therefore, FSE corrections in superfluid ^{4}He appear to be relevant even at so high q's.[12]

A direct comparison between theoretical and experimental dynamic structure factors is not possible due to the presence of instrumental resolution effects (IRE) in the experimental data acquisition process. It would be desirable, from a theoretical viewpoint, to remove the IRE inherent to the measured response, especially at high q where they become larger. However, the latter is an ill-posed problem due to the statistical noise of the data, and thus the only way to compare theory and experiment is by convoluting the theoretical $J(q,Y)$ with an instrumental resolution function $I(q,Y)$. At present, $I(q,Y)$ is obtained from a Monte Carlo simulation of the experimental setup, and in contrast to earlier models used in neutron scattering analysis, it is neither Gaussian nor symmetric around $Y = 0$, and is comparable in width and height to $R(q,Y)$ at those momenta.[4] The influence of $I(q,Y)$ in the response is sketched in Fig. 5 for $q = 23.1$ Å^{-1}. As one can see, the introduction of the IRE in the response (solid line) appreciably modifies $J(q,Y)$ (dashed line). The most important effect of $I(q,Y)$ is to quench the central peak reducing the effects of the FSE correction on $J_{IA}(Y)$, whereas the tails remain almost unchanged.

In Fig. 6, we present results of $J(q,Y)$ broadened by the IRE at different values of q in comparison with inelastic scattering data at $T = 0.34$ K from Ref. 4. There is an overall agreement between the predicted and the observed scattering data, the quality of the Gersch-Rodriguez theory being comparable to results provided by other theories[12,14] (see also Sec. V). It is worth to notice that all FSE theories are stressed when applied to intermediate q values. This is also apparent in our results, as one can see for the lowest q value reported in Fig. 6. Thus, whereas the experimental peak shifts its location to a small negative Y value, the theoretical one is shifted to so small positive values of Y that it is not appreciable in the figure.

The most relevant quantity in the calculation of $J(q,Y)$ is the momentum distribution $n(k)$ which completely determines the Compton profile $J_{IA}(Y)$. The influence of $n(k)$ in $J(q,Y)$ is shown in Fig. 7. The dashed and solid lines correspond to a Jastrow $n(k)$ [$n_J(k)$] and a Jastrow plus triplet $n(k)$ [$n_{JT}(k)$], respectively. The condensate fraction predicted by the two approximations are slightly different,
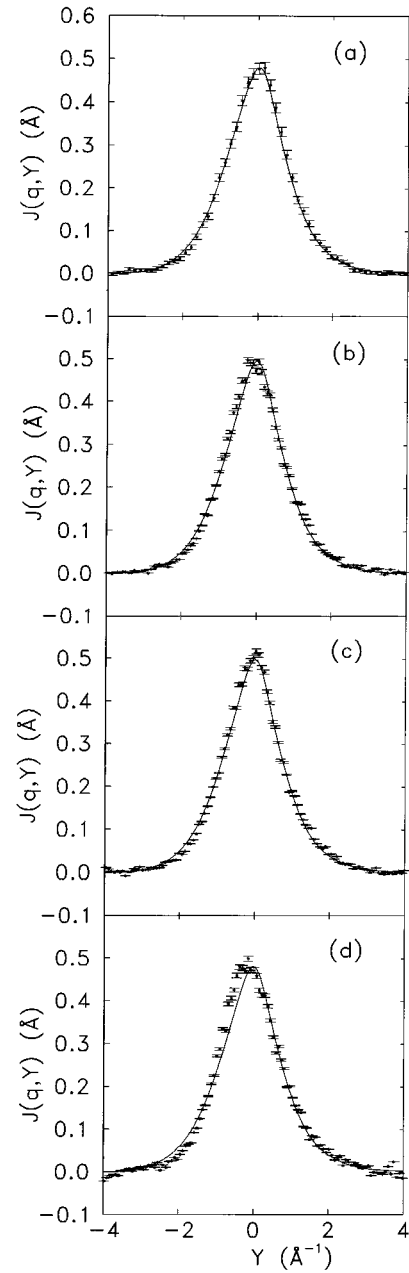

FIG. 6. Comparison of the predicted $J(q,Y)$ at (a) 23.1 Å^{-1}, (b) 17.9 Å^{-1}, (c) 15.0 Å^{-1}, and (d) 10.2 Å^{-1} with experimental data (points with error bars).

$n_0^J = 0.091$ and $n_0^{JT} = 0.082$. This reduction of n_0 produces a small decrease of strength in the peak of $J(q,Y)$ bringing our theoretical prediction closer to the experiment. A basic ingredient in the calculation of $R(q,Y)$ is the semidiagonal two-body density matrix, which in the framework of the HNC theory is given by[23]

$$\rho_2(\mathbf{r}_1,\mathbf{r}_2;\mathbf{r'}_1,\mathbf{r}_2)$$

$$= \rho\rho_1(r_{11'})g_{wd}(r_{12})g_{wd}(r_{1'2})\exp[A(\mathbf{r}_1,\mathbf{r}_2;\mathbf{r'}_1)], \quad (24)$$

where $\rho_1(r_{11'})$ is the one-body density matrix, $g_{wd}(r)$ is an auxiliary two-body radial distribution function, and
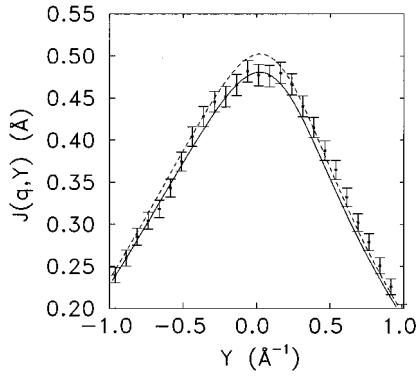
FIG. 7. Detail of the central peak of the response at $q=23.1$ Å^{-1} *as predicted using two different* $n(k)$'s. The solid and dashed lines correspond to $n_{JT}(k)$ and $n_J(k)$, respectively. The points with error bars are the experimental data.

$A(\mathbf{r}_1,\mathbf{r}_2;\mathbf{r}'_1)$ is the sum of the Abe diagrams. Notice that the structure of ρ_2 allows for the exact cancellation of ρ_1 in Eq. (14). As the explicit dependence of ρ_2 in n_0 is introduced in ρ_1, the influence of n_0 in $R(q,Y)$ is almost negligible. We have verified that the inclusion of three-body correlations does not appreciable modify the structure of $R(q,Y)$. Consequently, three-body correlations can be omitted in the calculation of $R(q,Y)$. In a further step, we have also studied the influence of the Abe diagrams using a Jastrow wave function. As is well known, it is not possible to calculate $A(\mathbf{r}_1,\mathbf{r}_2,\mathbf{r}'_1)$ exactly but a good estimation of its contribution can be obtained through the scaling approximation.[27] The inclusion of the Abe diagrams in Eq. (24) using the scaling approximation produce negligible effects in the final form of $R(q,Y)$. In fact, the Abe terms, which quickly vanish when the interparticle separation increases, only modify the structure of ρ_2 when coordinates 1, 1′, and 2 are very close to each other. These small changes in ρ_2 are then suppressed when integrated to obtain $R(q,t)$. Furthermore, one can slightly change the functions $g_{wd}(r)$ and no influences in $R(q,Y)$ are observed. This fact, which will be explicitly commented in Sec. V, points to the relevance of the functional decomposition of ρ_2 rather than the exact form of the functions entering in it.

IV. SUM RULES

In this section we study the sum rules satisfied by the Gersch-Rodriguez FSE broadening function $R(q,Y)$. From the relation

$$J(q,Y)=\int_{-\infty}^{\infty} dY' J_{\mathrm{IA}}(Y')R(q,Y-Y'), \qquad (25)$$

and the first sum rules of both $J_{\mathrm{IA}}(Y)$ and the incoherent part of $J(q,Y)$, an equivalent set of Y-weighted integrals for $R(q,Y)$ can be derived.[12] Notice that Eq. (25) can be taken as a possible definition of $R(q,Y)$ provided that q is large enough for the coherent part of $J(q,Y)$ to be negligible. These sum rules are model independent, and so any suitable convolutive FSE broadening function must fulfill them. The first sum rules of $R(q,Y)$ are

$$m_0^R(q)=\int_{-\infty}^{\infty} dY R(q,Y)=1,$$

$$m_1^R(q)=\int_{-\infty}^{\infty} dY Y R(q,Y)=0,$$

$$m_2^R(q)=\int_{-\infty}^{\infty} dY Y^2 R(q,Y)=0,$$

$$m_3^R(q)=\int_{-\infty}^{\infty} dY Y^3 R(q,Y)=\frac{m}{2q^3}\rho \int d\mathbf{r}g(r)(\mathbf{q}\cdot\boldsymbol{\nabla})^2 V(r).$$
(26)

As we are only considering the incoherent part of the response, $m_0^R(q)$ is 1 at any q. Both the first and second moments of $R(q,Y)$ vanish because the impulse approximation exactly fulfills the incoherent sum rules. Finally, the third moment of $R(q,Y)$ is expressed in terms of the two-body radial distribution function $g(r)$ and the interatomic potential $V(r)$, which are not included in $J_{\mathrm{IA}}(Y)$.

Relations (26) are exact and partially define the behavior of $R(q,Y)$. Therefore, one can use them to check the accuracy of $R(q,Y)$ calculated using different approximations. In the Gersch-Rodriguez theory, the sum rules analysis can be analytically performed. In fact, expressions for the sum rules can be easily derived from the time derivatives of $R(q,t)$ at $t=0$,

$$m_k^R(q)=\frac{1}{i^k v_q^k}\frac{d^k}{dt^k}R(q,t)\bigg|_{t=0}. \qquad (27)$$

Performing a McLaurin expansion of $R(q,t)$, Eq. (14), the different coefficients of the series are directly related to the Y-weighted sum rules. In this way, one obtains the relations

$$m_0^{R,\mathrm{GR}}(q)=1,$$

$$m_1^{R,\mathrm{GR}}(q)=0,$$

$$m_2^{R,\mathrm{GR}}(q)=0,$$

$$m_3^{R,\mathrm{GR}}(q)=\frac{2m}{q^3\rho}\int d\mathbf{r}\,\rho_2(\mathbf{r},0;\mathbf{r})(\mathbf{q}\cdot\boldsymbol{\nabla})^2 V(r)$$

$$+\frac{3m}{q^3\rho}\int d\mathbf{r}[(\mathbf{q}\cdot\boldsymbol{\nabla})V(r)][(\mathbf{q}\cdot\boldsymbol{\nabla}_\mathbf{x})\rho_2(\mathbf{r},0;\mathbf{x})]_{\mathbf{x}=\mathbf{r}}$$
(28)

where $m_k^{R,\mathrm{GR}}(q)$ stand for the Y-weighted integral of the FSE function in Gersch-Rodriguez theory. Integrating by parts the second term of $m_3^{R,\mathrm{GR}}(q)$, and taking into account general symmetry properties of ρ_2, one can express $m_3^{R,\mathrm{GR}}(q)$ in the following way:

$$m_3^{R,\mathrm{GR}}(q)=\frac{m}{2q^3\rho}\int d\mathbf{r}\,\rho_2(\mathbf{r},0;\mathbf{r})(\mathbf{q}\cdot\boldsymbol{\nabla})^2 V(r). \qquad (29)$$
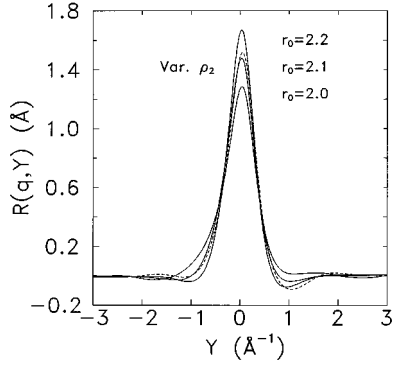
FIG. 8. Comparison of $R(q,Y)$ calculated using the Gersch-Rodriguez ρ_2 with different values of r_0 (solid lines) and the variational ρ_2 (dashed line).

As the diagonal part of ρ_2 is $\rho^2 g(r)$, the analytical expression of m_3^R is recovered. Therefore, the zero, first, second, and third moments of $R(q,Y)$ are exactly fulfilled in the Gersch-Rodriquez theory.

Nevertheless, the exact ρ_2 is not known, and the use of an approximation can produce numerical differences between Eqs. (29) and (26). In fact, we have checked that the inclusion of the Abe terms in the variational ρ_2 defined in Eq. (24) is crucial in reproducing $g(r)$ in its diagonal part, and consequently $m_3^R(q)$.

V. COMPARISON WITH OTHER FSE THEORIES

FSE theories can be classified in different groups depending on the way they incorporate the corrections to the IA. The two most important groups are, on one hand, convolutive theories in which the total response is expressed as a convolution of $J_{IA}(Y)$ and $R(q,Y)$ and, on the other, additive theories where the leading FSE corrections are summed up to the IA. Examples of theories belonging to the first class are those of Silver[12] or Carraro and Koonin.[14] An example of additive theory is that originally derived by Gersch, Rodriguez and Smith,[8] which was next generalized by Rinat[13] to treat also hard core potentials.

Gersch-Rodriguez formalism was the first in predicting convolutive FSE corrections. Silver's and Carraro and Koonin's theories appeared some years after. In this section, we present a comparison between their results and our predic-
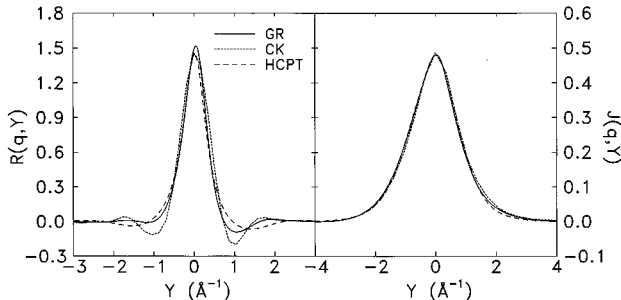

FIG. 9. Comparison between Gersch-Rodriguez, Silver, and Carraro and Koonin results for both $R(q,Y)$ and $J(q,Y)$ at $q=23.1$ Å^{-1}.

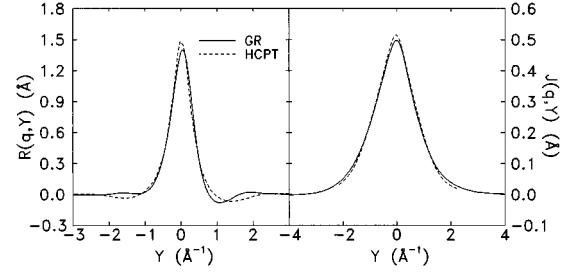tions obtained in the framework of the Gersch-Rodriguez theory.

In the Gersch-Rodriguez theory $R(q,Y)$ is formulated in terms of the semidiagonal two-body density matrix of the system. In the present work, a variational ansatz for this quantity has been employed and discussed, but at the time the formalism was developed only a qualitative description of ρ_2 was available. This led the original authors to use a form of ρ_2 based on a Hartree-Fock approximation and the Schwartz inequality[8]

$$\rho_2(\mathbf{r}_1,\mathbf{r}_2;\mathbf{r'}_1,\mathbf{r}_2)=\rho\rho_1(r_{11'})\sqrt{g(r_{12})g(r_{1'2})}, \quad (30)$$

$\rho_1(r)$ being the one-body density matrix and $g(r)$ the two-body radial distribution function. At that time, detailed microscopic calculations of $g(r)$ were not available, so they had to approximate it. The form selected for the radial distribution function was simply a step function

$$g(r)=\theta(r-r_0), \quad (31)$$

with a parameter r_0 to mimic the radius of the hole of $g(r)$. Originally, r_0 was taken as a fitting parameter. However, theoretical arguments brought them to fix its value to $r_0=2.5$ Å.[10] With this prescription, Gersch and Rodriguez predicted a $J(q,Y)$ that visibly overestimates the measured strength of the response around its maximum. This failure was later discussed and partially attributed to a somewhat excessively simplified approximation to the problem.[12] Nevertheless, this discrepancy seems to be eliminated by choosing a different value of r_0. In order to show this feature, several calculations using Eqs. (31) and (32) with different values of r_0 have been performed. In Fig. 8, results for $R(q,Y)$ with r_0 equal to 2.0, 2.1, and 2.2 Å are depicted and compared to $R(q,Y)$ computed with the variational ρ_2. Even though the behavior of the tails of $R(q,Y)$ in the Gersch-Rodriguez approximation of ρ_2 is different from the one of $R(q,Y)$ with the variational two-body density matrix, the height and width of both peaks are in good agreement for a value of r_0 laying between 2.1 and 2.2 Å. Then, a proper choice of r_0 in the simple Gersch-Rodriguez model for ρ_2 produces accurate results, provided that the height and width of the central peak are the most important features of the FSE broadening function.

We have compared our results for $R(q,Y)$ and $J(q,Y)$ with those obtained by Silver[12] and Carraro and Koonin.[14] Figures 9, 10, and 11 show $R(q,Y)$ and $J(q,Y)$ in Gersch-Rodriguez (GR), Silver (HCPT), and Carraro and Koonin
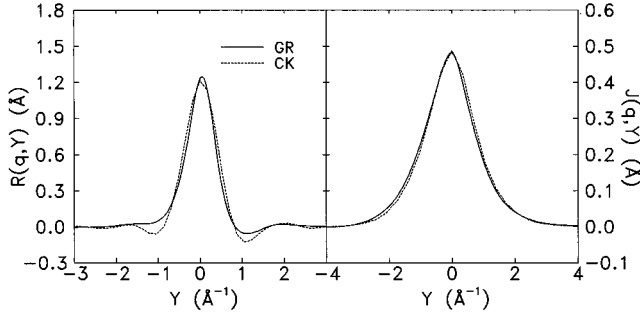
FIG. 11. Comparison between Gersch-Rodriguez and Carraro and Koonin results for both $R(q,Y)$ and $J(q,Y)$ at $q = 10.2$ Å^{-1}.

(CK) theories for three values of q, 23.1, 15.5, and 10.2 Å^{-1}. The FSE function $R(q,Y)$ is slightly different in the three theories, though both the height and width of the central peak are quite similar. The tails of the FSE broadening function show a different behavior, although they quickly vanish as $|Y|$ increases. Despite of the discrepancies in $R(q,Y)$, the predicted responses are nearly the same at $q = 23.1$ Å^{-1} and in good agreement with the experimental data. As q is lowered, the deficiencies of the FSE theories show up but $J(q,Y)$ is still reasonably well described at $q = 15.5$ Å^{-1}. For the lowest q value, $q = 10$ Å^{-1} (Fig. 11), the theoretical responses move away from experiment, and in particular do not present the small shift of the peak to negative Y values (see also Fig. 6). Then, even for intermediate q values, the Gersch–Rodriguez theory reproduces the dynamic structure function as precisely as other existing theories for the FSE.

VI. SUMMARY AND CONCLUSIONS

In this work, final state effects on the density response of superfluid ^{4}He have been studied in the framework of the Gersch-Rodriguez theory using a realistic description of the ground state of the liquid. The response is predicted as the convolution product of the Compton profile $J_{IA}(Y)$ and the FSE broadening function $R(q,Y)$.

Two quantities describing the ground state of the system are needed. The first one is the momentum distribution $n(k)$, which completely determines $J_{IA}(Y)$. The second one is the semidiagonal two-body density matrix, which enters in the Gersch-Rodriguez form of $R(q,Y)$.

$J_{IA}(Y)$ has two terms, one corresponding to the noncondensate part of $n(k)$ and another given by $n_0\delta(Y)$. This splitting produces, after convoluting with $R(q,Y)$, a total response which is also the sum of two terms, corresponding to the condensate and noncondensate contributions. The former is linear in n_0 and mostly affects $J(q,Y)$ around $Y = 0$. The latter is much less affected by FSE, although the effects are nonnegligible. We have verified that Gersch-Rodriguez theory gives accurate results when proper forms for the one- and two-body density matrices are used. A variational ρ_2 obtained in the HNC framework accurately reproduces the experimental response at high q's. Furthermore, we have checked that the functional decomposition of ρ_2 is very important in the calculation of $R(q,Y)$. Simple models conserving the variational functional form can also produce a good estimation of the response.

Our results are comparable to other calculations using more recent convolutive FSE theories. None of the theories correctly accounts for the observed response when q is lowered below about 10 Å^{-1}. Further improvements could arise when higher order terms in the Gersch-Rodriguez cumulant expansion are considered or the time dependence of the particle coordinates is taken into account.

[1] P.C. Hohenberg and P.M. Platzman, Phys. Rev. **152**, 198 (1966).

[2] *Momentum Distributions*, edited by R.N. Silver and P.E. Sokol (Plenum, New York, 1989).

[3] *Neutron Scattering*, edited by D.L. Price and K. Skold, Methods of Experimental Physics Vol. 23 (Academic, New York, 1987).

[4] T.R. Sosnick, W.M. Snow, P.E. Sokol, and R.N. Silver, Europhys. Lett. **9**, 707 (1989).

[5] T.R. Sosnick, W.M. Snow, and P.E. Sokol, Phys. Rev. B **41**, 11 185 (1990).

[6] T.R. Sosnick, W.M. Snow, R.N. Silver, and P.E. Sokol, Phys. Rev. B **43**, 216 (1991).

[7] Y. Wang and P.E. Sokol, Phys. Rev. Lett. **72**, 1040 (1994).

[8] H.A. Gersch, L.J. Rodriguez, and P.N. Smith, Phys. Rev. A **5**, 1547 (1972).

[9] H.A. Gersch and L.J. Rodriguez, Phys. Rev. A **8**, 905 (1973).

[10] L.J. Rodriguez, H.A. Gersch, and H.A. Mook, Phys. Rev. A **9**, 2085 (1974).

[11] V.F. Sears, Phys. Rev. B **30**, 44 (1984).

[12] R.N. Silver, Phys. Rev. B **37**, 3794 (1988); **38**, 2283 (1988); **39**, 4022 (1989).

[13] A.S. Rinat, Phys. Rev. B **40**, 6625 (1989); **42**, 9944 (1990), and references therein.

[14] C. Carraro and S.E. Koonin, Phys. Rev. Lett. **65**, 2792 (1990); Phys. Rev. B **41**, 6741 (1990).

[15] H.R. Glyde, Phys. Rev. B **50**, 6726 (1994).

[16] A. Belic and V.R. Pandharipande, Phys. Rev. B **45**, 839 (1992).

[17] J. Boronat, F. Dalfovo, F. Mazzanti, and A. Polls, Phys. Rev. B **48**, 7409 (1993).

[18] S.W. Lovesey, *Theory of Neutron Scattering from Condensed Matter* (Oxford University Press, Oxford, 1984), Vol. 1.

[19] G.B. West, Phys. Rep. **18C**, 263 (1975).

[20] S. Fantoni, Nuovo Cimento A **44**, 191 (1978).

[21] E. Manousakis, V.R. Pandharipande, and Q.N. Usmani, Phys. Rev. B **43**, 13 587 (1991).

[22] J. Boronat, Ph.D. thesis, University of Barcelona, 1991.

[23] M.L. Ristig and J.W. Clark, Phys. Rev. B **40**, 4355 (1989); M.L. Ristig, Nucl. Phys. A **317**, 163 (1979).

[24] R.A. Aziz, V.P.S. Nain, J.S. Carley, W.L. Taylor, and G.T. McConville, J. Chem. Phys. **70**, 4330 (1979).

[25] J. Boronat and J. Casulleras, Phys. Rev. B **49**, 8920 (1994).

[26] P. Whitlock and R.M. Panoff, Can. J. Phys. **65**, 1409 (1987).

[27] Q.N. Usmani, B. Friedman, and V.R. Pandharipande, Phys. Rev. B **25**, 4502 (1982).